Splashing of Large Helium Nanodroplets upon Surface Collisions

Paul Martini,[1,2] Simon Albertini,[1,3] Felix Laimer,[1] Miriam Meyer,[1] Michael Gatchell,[1,2] Olof Echt,[1,4] Fabio Zappa,[1,5,*] and Paul Scheier[1]

[1]*Institut für Ionenphysik und Angewandte Physik, Universität Innsbruck, A-6020 Innsbruck, Austria*
[2]*Department of Physics, Stockholm University, 106 91 Stockholm, Sweden*
[3]*Management Center Innsbruck, Department Biotechnology & Food Engineering, A-6020 Innsbruck, Austria*
[4]*Department of Physics, University of New Hampshire, Durham, New Hampshire 03824, USA*
[5]*Departamento de Física, Universidade Federal de Juiz de Fora, MG 36036-900 Minas Gerais, Brazil*

(Received 25 March 2021; revised 15 July 2021; accepted 12 November 2021; published 23 December 2021)

In the present work we observe that helium nanodroplets colliding with surfaces can exhibit splashing in a way that is analogous to classical liquids. We use transmission electron microscopy and mass spectrometry to demonstrate that neutral and ionic dopants embedded in the droplets are efficiently backscattered in such events. High abundances of weakly bound He-tagged ions of both polarities indicate a gentle extraction mechanism of these ions from the droplets upon collision with a solid surface. This backscattering process is observed for dopant particles with masses up to 400 kilodaltons, indicating an unexpected mechanism that effectively lowers deposition rates of nanoparticles formed in helium droplets.

DOI: 10.1103/PhysRevLett.127.263401

The interaction of droplets with surfaces is the basis of numerous technological applications, using a great variety of liquids [1,2]. In the field of mass spectrometry, for instance, it can be used as a means to transfer to the gas phase, in a nondestructive way, fragile molecules that are either inside the droplets [3] or on the surface [4,5].

Helium nanodroplets (HNDs), although consisting of a quite particular and unusual superfluid liquid, have also been the target of a lot of interest and found many applications in basic science as a unique matrix to produce aggregates of molecules or atoms at temperatures below 1 K [6]. Experiments with HNDs have included spectroscopy of cold neutral [7,8] and charged dopants [9], x-ray diffraction of pristine and doped HNDs [10,11] as well as the deposition of dopant nanoparticles (NPs) [12,13], nanowires [14–17], core-shell NPs [18,19], and NPs functionalized with fluorophores [20]. In order to ionize the droplets, a wide range of processes have been utilized, from electron ionization [6,21] to photoionization utilizing free electron lasers [22,23].

It has been known, since the pioneering work of Gspann [24], that van der Waals clusters can bounce and to some extent survive the collision with a surface. In agreement with these results, Schöllkopf *et al.* [25] observed that large clusters avoid complete destruction when colliding with a grating, with smaller fragments surviving the impact. Nevertheless, very little has been reported about the fate of dopants inside HNDs after such collisions. Recently, the soft landed deposition of nanoparticles or nanowires formed in large neutral HNDs was explained by the evaporation of helium atoms and a flattening of the remaining HND, cushioning the impact and preventing the NPs from being backscattered [13,26–29].

In order to investigate whether the doping material inside helium nanodroplets is indeed totally deposited on surfaces, we prepared a sample holder for transmission electron microscopy (TEM) grids schematically represented in Fig. 1(a). Sample G1 is placed in the path of a neutral doped droplet beam, while sample G2 is positioned in a perpendicular orientation without a direct line of sight. The HND beam used in our experiment consists of large HNDs (containing $> 10^{10}$ atoms) formed at 5.25 K nozzle temperature and 30 MPa helium stagnation pressure. These are then doped in a differentially pumped chamber by sequential pickup of Bi atoms that are evaporated in a resistively heated oven (925 K). The sample surfaces consist of Quantifoil™ (R2/2, UT, 400 mesh, copper) TEM grids and are imaged with a Zeiss Libra 120 EFTEM. Figure 1(b) presents TEM images of samples G1 and G2 after a deposition time of 1 hour. As we can see, NPs are present on both samples, not only on the one directly facing the helium beam. The sizes of the particles averaged 4.83(4) nm for G1 (0°) and 5.13(8) nm for G2 (90°) (obtained with CellProfiler™ [30], see Supplemental Material [31]). The surprising coverage of the TEM grid at 90° upon neutral deposition is of particular interest as it points to the possibility that more complex phenomena come into play when a droplet collides with a surface.

Attempts at performing similar experiments with charged droplets faced the difficulty that the NPs obtained were generally much smaller than in the neutral case, making imaging less reliable. Furthermore, the possibility that some NPs formed in the droplets might not get ionized could lead to ambiguous results. Therefore we chose to use mass spectrometry to study the products of charged

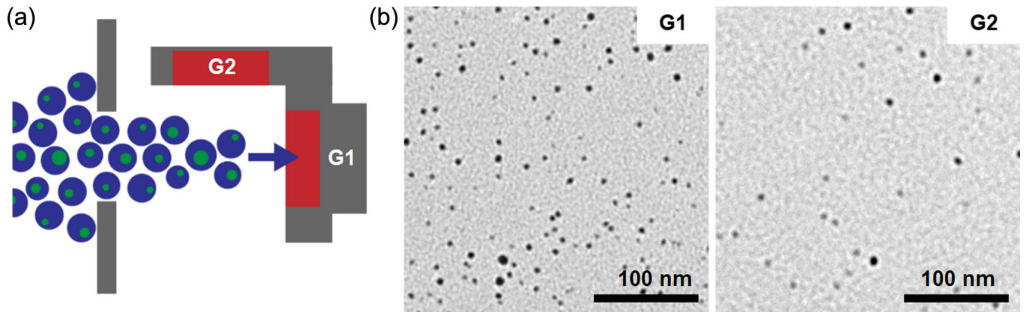

FIG. 1. (a) Scheme of the positioning of the primary grid (G1) and the secondary grid (G2). Doped HNDs collide at normal incidence with G1. G2 is mounted perpendicular to G1 at a distance of about 1.5 mm. (b) TEM images from grids positioned at G1 and at G2.

droplets impinging on a surface, with the hope that neutralization of charge at the surface would not be the sole observable process. We modified a setup previously used in most of our studies with HNDs, depicted in Fig. 2(a) [32]. With that previous arrangement we have been able to study the chemical reactivity of several atomic and molecular species at low temperatures and, in some particular cases, perform action spectroscopy of helium-tagged molecules of astrophysical interest [33,34]. Having identical ion optics and the mass spectrometer of previous experiments, we can expect that the modified setup permits a direct comparison with previous results. In the present Letter, the following modifications are introduced [see Fig. 2(b)]: first, the order of ionization and pickup is reversed, with the purpose of taking advantage of the high yield of dopant ions observed in Ref. [35]; second, a polished stainless-steel surface is introduced in the path of the HND beam, inside the "ion block" of the original ion source and in a position similar to where electrons interact with stagnant gas or neutral cluster beams in the original

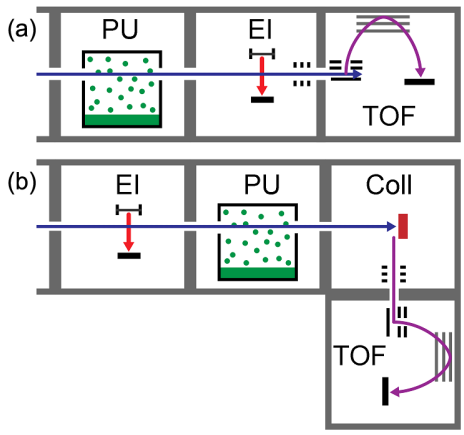

FIG. 2. (a) Schematic illustration of the original experimental configuration used to study ions generated by electron ionization of neutral, doped helium nanodroplets. (b) Modified configuration for the investigation of ions ejected from preionized and doped HNDs colliding with a metal surface (Coll). PU is the pickup cell, TOF is the orthogonal extraction reflectron time of flight mass spectrometer, and EI is the electron ionization gun.

configuration (see Supplemental Material [31]). For convenience, the orientation of the target surface was chosen so that the HNDs collide at normal incidence. The potential applied to the surface, between 5 and 20 V (negative for anions), corresponds to the usual value that is used to set an appropriate kinetic energy of the ions when they enter the pulsing region of the time of flight (TOF) spectrometer. The potential does not appreciably change the kinetic energy with which the HNDs collide with the surface, because that energy is predominantly determined by the supersonic expansion conditions. In the present experiment all components of the ion source, including the collision surface, are at room temperature.

The choice of the dopant substance and ionizing conditions are determined by the availability and quality of data obtained with the original configuration. Therefore, C_{60} is chosen as our sample that is vaporized with an oven operated between 575 and 625 K. An electron energy of about 22 eV is used to produce anions, and about 57 eV for cations. The electron current is kept at 350 μA for all experiments, which implies multiple hits and multiply charging of the HNDs. The cryostat is operated between 9.6 and 10 K, and the helium stagnation pressure is kept between 25 and 29 bar. The raw mass spectra are available in the Supplemental Material [31], and here we shall present processed ion yields obtained by the software IsotopeFit, which accounts for isotopic patterns and assigns appropriate contributions of isobaric ions [36].

To our surprise the collision of doped, charged HNDs with the surface produces an excellent signal that is more intense than the one obtained in the original configuration, as can be seen in Fig. 3 where we focus on the yield of He-tagged C_{60} cations or anions. Most notably, the intensity of He-tagged ions from the surface collision setup is increased by about 2 orders of magnitude for cations and more than 3 orders of magnitude for anions over the old setup. Furthermore, the ratio of bare monomeric C_{60} vs He-tagged C_{60} is decreased in the surface collision setup by a similar amount, indicating a more efficient production and extraction of cold, helium-solvated ions in the surface collision setup. Pronounced intensity drops visible at $n = 32$ and $n = 60$ are well known and have previously been assigned

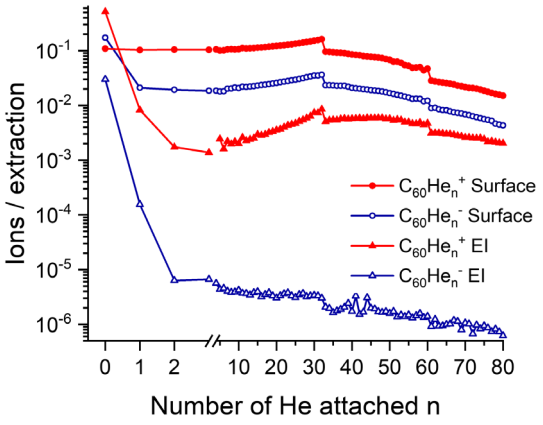

FIG. 3. Comparison of He attachment distributions on C_{60} ions produced with the two different configurations of the experimental setup. Ions obtained via surface collisions of multiply charged HNDs doped with C_{60} [see Fig. 2(b)] are shown as circles and ions formed upon electron ionization (EI) of neutral HNDs doped with C_{60} [see Fig. 2(a)] are indicated as triangles. An increase in He-tagged ion production and/or detection in the surface collision setup by several orders of magnitude can be observed. In order to compare ion yields of different polarities (measured with different repetition rates of the TOF cycle) they are presented as ions per TOF extraction pulse.

to the completion of a commensurate layer of He on C_{60} and the closure of the first solvation layer, respectively [9,37,38].

Care must be taken in the interpretation of these spectra. There could be two possibilities: either the ions observed come from the fragmentation of the droplets themselves or the impinging droplets remove and ionize material from the surface, deposited by previous droplets, akin to what has been demonstrated previously with argon clusters [4]. In order to exclude the second possibility, we have performed experiments with undoped, ionized droplets colliding with a precoated surface containing various types of substances. No ions were observed to be ejected from the surface, only pristine helium cluster ions.

To rationalize these findings we first take into account that the velocity of HNDs in our experiment ranges between 120 and 250 m/s [39]. These velocities are larger than the Landau critical velocity in HNDs [40], which is an upper limit for superfluidity. Therefore, the helium can be expected to behave like a normal liquid during the surface collision. The dimensionless Weber number, which is defined as

$$W_e = \frac{\rho d v_\perp^2}{\sigma}$$

can be used to describe the collision of droplets with a solid surface [41], with ρ, d, and σ the density, diameter, and surface tension of the droplets, respectively, and $v_\perp^2$ the velocity component of impinging droplets orthogonal to the surface. Splashing of droplets is observed upon collisions onto dry smooth solid surfaces for Weber numbers larger than 1000 for various liquids [42]. In our case W_e turns out to be 1670, which suggests possible splashing and breakup into secondary droplets, backscattering from the surface.

Following the splashing hypothesis, we can understand the higher yield of dopant ions, when compared to the original setup, as a consequence of the inverted ionization-doping sequence. In the original setup a relatively small fraction of the generated ions could be detected, namely only those that were ejected from HNDs within a few microseconds after the electron impact, and which were light enough to be effectively guided to the mass spectrometer by low voltage electrostatic lenses (< 250 V). Such a detection scheme is blind to ions that remain trapped inside the large HNDs. In the modified setup, each charge carrier within the droplet acts as a separate nucleation center [35], and the ionized dopants are stable inside the HNDs even when subjected to electrostatic forces (which are due to either multiple charging within the droplet itself or external fields). While in Ref. [35] ions were liberated from the droplets via collisions with helium gas inside a hexapole ion guide, in the present case the ions are liberated when the droplets collide with the surface. The splashing of the droplets prevents the direct interaction of dopant ions with the metallic surface, which would otherwise lead to neutralization via electron transfer. This explanation is corroborated by comparing relative ion yields of opposite mass spectrometer polarities when identical conditions for the supersonic expansion and doping are used, and only the electron energy is changed (See Figure S7 in the Supplemental Material [31]). We observe that the probability of obtaining $(C_{60})_m^{\pm}$ clusters with larger m increases significantly as we go from positive ions to negative ions, consistent with the expected lower charge state of negative HNDs [21,43]. Further investigation will be necessary to determine the importance of surface composition, incident angle, and other parameters on the kinematics of the scattered products. New experiments designed to answer these questions are being planned.

Incidentally, the high yield of He-tagged anions makes action spectroscopy of these species feasible for the first time. Until now, spectroscopy of anions embedded in HNDs was only achieved via evaporation of the HNDs by the intense light of a free electron laser upon multiphoton absorption of an anionic dopant [44]. Figure 4 shows the absorption spectrum of C_{60}^- obtained via the formation of the photo product (blue line). The spectrum was produced by merging the light of a tunable pulsed laser (EKSPLA NT 242) with the ion beam containing He-tagged fullerene anions. Synchronization between the laser pulses (1 kHz repetition rate) and the TOF (10 kHz extraction rate) enables simultaneous measurements of mass spectra with laser on and off. For comparison the figure also shows the photo absorption of C_{60}^- ions

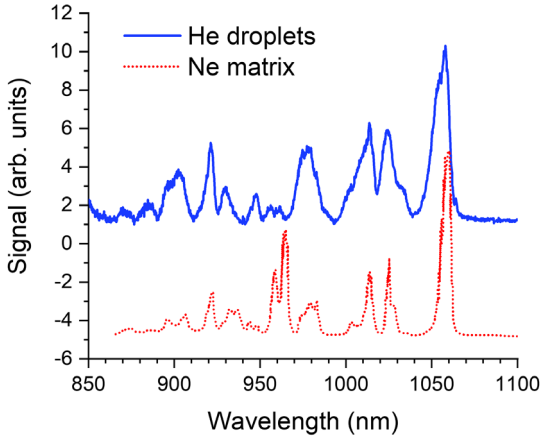

FIG. 4. Photoabsorption spectra of $C_{60}He_n$ anions. The blue solid line shows the increase of the photo product C_{60}^- upon photodissociation of C_{60} anions solvated with up to a few hundred He atoms. The red dotted line represents a matrix isolation spectrum of C_{60}^- embedded in solid neon [45].

deposited in a solid neon matrix (red dotted line) [45]. The agreement between the two absorption spectra is reasonably good, keeping in mind that contributions from cationic and neutral fullerenes in solid neon can lead to additional absorption lines. Furthermore, the interaction of C_{60}^- with neighboring He or Ne atoms leads to solvent dependent matrix shifts [9]. Identification of the peaks requires careful analysis and support from theoretical calculations, which are beyond the scope of the present Letter.

To summarize, we have investigated the scattering of HND dopants from surfaces both for high mass neutral nanoparticles ($m \leq 400$ kDa) via TEM imaging, and low mass ionic species ($m < 10$ kDa) via TOF mass spectrometry. We demonstrated that doped helium droplets colliding with a surface effectively behave like an ordinary liquid, protecting dopants from directly interacting with the surface, therefore hindering charge neutralization. Among other applications, the high yield of cold dopant ions liberated in this process, for both polarities, allows for unprecedented flexibility in the preparation of action spectroscopy experiments with helium-tagged molecular species. Furthermore, the TEM images revealed that when HNDs are used as a cushion for soft-landing NPs on a substrate the partial backscattering of large NPs has to be considered.

The authors acknowledge W. Salvenmoser for valuable input on theoretical and practical aspects of TEM imaging. The present work was supported by the Austrian Science Fund, FWF, Projects No. P31149 and No. I4130, the Swedish Research Council, Projects No. 2016-06625 and No. 2020-03104, and the K-Regio project "FAENOMENAL," Project No. EFRE 2016-4, funded by the Tyrolian government and the European Regional Development Fund. F. Z. acknowledges support from CNPq. This article is based upon work from COST Action CA18212—Molecular Dynamics in the GAS phase (MD-GAS), supported by COST (European Cooperation in Science and Technology).

P. M. and S. A. contributed equally to this work.

*fabio.zappa@uibk.ac.at

[1] A. Yarin, Annu. Rev. Fluid Mech. **38**, 159 (2006).
[2] M. Rein, Fluid Dyn. Res. **12**, 61 (1993).
[3] Z. Takats, J. M. Wiseman, and R. G. Cooks, J. Mass Spectrom. **40**, 1261 (2005).
[4] A. Delcorte, V. Delmez, C. Dupont-Gillain, C. Lauzin, H. Jefford, M. Chundak, C. Poleunis, and K. Moshkunov, Phys. Chem. Chem. Phys. **22**, 17427 (2020).
[5] S. N. Sun and H. M. Urbassek, J. Phys. Chem. B **115**, 13280 (2011).
[6] A. Mauracher, O. Echt, A. M. Ellis, S. Yang, D. K. Bohme, J. Postler, A. Kaiser, S. Denifl, and P. Scheier, Phys. Rep.-Rev. Sect. Phys. Lett. **751**, 1 (2018).
[7] A. S. Chatterley, L. Christiansen, C. A. Schouder, A. V. Jorgensen, B. Shepperson, I. N. Cherepanov, G. Bighin, R. E. Zillich, M. Lemeshko, and H. Stapelfeldt, Phys. Rev. Lett. **125**, 013001 (2020).
[8] B. Thaler, M. Meyer, P. Heim, and M. Koch, Phys. Rev. Lett. **124**, 115301 (2020).
[9] M. Kuhn, M. Renzler, J. Postler, S. Ralser, S. Spieler, M. Simpson, H. Linnartz, A. G. Tielens, J. Cami, A. Mauracher, Y. Wang, M. Alcami, F. Martin, M. K. Beyer, R. Wester, A. Lindinger, and P. Scheier, Nat. Commun. **7**, 13550 (2016).
[10] S. M. O. O'Connell, P. Rico Mayro Tanyag, D. Verma, C. Bernando, W. Pang, C. Bacellar, C. A. Saladrigas, J. Mahl, B. W. Toulson, Y. Kumagai, P. Walter, F. Ancilotto, M. Barranco, M. Pi, C. Bostedt, O. Gessner, and A. F. Vilesov, Phys. Rev. Lett. **124**, 215301 (2020).
[11] L. F. Gomez *et al.*, Science **345**, 906 (2014).
[12] A. Schiffmann, T. Jauk, D. Knez, H. Fitzek, F. Hofer, F. Lackner, and W. E. Ernst, Nano Res. **13**, 2979 (2020).
[13] E. Loginov, L. F. Gomez, and A. F. Vilesov, J. Phys. Chem. A **115**, 7199 (2011).
[14] S. Yang, C. Feng, D. Spence, A. M. Al Hindawi, E. Latimer, A. M. Ellis, C. Binns, D. Peddis, S. S. Dhesi, L. Zhang, Y. Zhang, K. N. Trohidou, M. Vasilakaki, N. Ntallis, I. MacLaren, and F. M. de Groot, Adv. Mater. **29**, 1604277 (2017).
[15] E. Latimer, D. Spence, C. Feng, A. Boatwright, A. M. Ellis, and S. Yang, Nano Lett. **14**, 2902 (2014).
[16] D. Spence, E. Latimer, C. Feng, A. Boatwright, A. M. Ellis, and S. Yang, Phys. Chem. Chem. Phys. **16**, 6903 (2014).
[17] M. Schnedlitz, M. Lasserus, D. Knez, A. W. Hauser, F. Hofer, and W. E. Ernst, Phys. Chem. Chem. Phys. **19**, 9402 (2017).
[18] G. Haberfehlner, P. Thaler, D. Knez, A. Volk, F. Hofer, W. E. Ernst, and G. Kothleitner, Nat. Commun. **6**, 8779 (2015).
[19] A. Boatwright, C. Feng, D. Spence, E. Latimer, C. Binns, A. M. Ellis, and S. Yang, Faraday Discuss. **162**, 113 (2013).
[20] R. Messner, W. E. Ernst, and F. Lackner, J. Phys. Chem. Lett. **12**, 145 (2021).

[21] F. Laimer, L. Kranabetter, L. Tiefenthaler, S. Albertini, F. Zappa, A. M. Ellis, M. Gatchell, and P. Scheier, Phys. Rev. Lett. **123**, 165301 (2019).
[22] A. C. LaForge, M. Shcherbinin, F. Stienkemeier, R. Richter, R. Moshammer, T. Pfeifer, and M. Mudrich, Nat. Phys. **15**, 247 (2019).
[23] M. Mudrich *et al.*, Nat. Commun. **11**, 112 (2020).
[24] J. Gspann and G. Krieg, J. Chem. Phys. **61**, 4037 (1974).
[25] W. Schöllkopf, J. P. Toennies, T. Savas, and H. I. Smith, J. Chem. Phys. **109**, 9252 (1998).
[26] L. F. Gomez, E. Loginov, and A. F. Vilesov, Phys. Rev. Lett. **108**, 155302 (2012).
[27] R. Fernández-Perea, L. F. Gómez, C. Cabrillo, M. Pi, A. O. Mitrushchenkov, A. F. Vilesov, and M. P. de Lara-Castells, J. Phys. Chem. C **121**, 22248 (2017).
[28] W. E. Ernst and A. W. Hauser, Phys. Chem. Chem. Phys. **23**, 7553 (2021).
[29] S. Yang, A. M. Ellis, D. Spence, C. Feng, A. Boatwright, E. Latimer, and C. Binns, Nanoscale **5**, 11545 (2013).
[30] M. R. Lamprecht, D. M. Sabatini, and A. E. Carpenter, BioTechniques **42**, 71 (2007).
[31] See Supplemental Material at http://link.aps.org/supplemental/10.1103/PhysRevLett.127.263401 for the recorded and fitted mass spectra, a comparison of ion yields for 4 different experimental configurations, mass spectra of positively and negatively charged C60 cluster ions indicating that charges can act as nucleation centers, the acquired TEM images with the corresponding analysis and a simulation illustrating the path of the ions after the collisions of the HNDs with a surface.
[32] H. Schöbel, P. Bartl, C. Leidlmair, S. Denifl, O. Echt, T. D. Märk, and P. Scheier, Eur. Phys. J. D **63**, 209 (2011).
[33] S. Spieler, M. Kuhn, J. Postler, M. Simpson, R. Wester, P. Scheier, W. Ubachs, X. Bacalla, J. Bouwman, and H. Linnartz, Astrophys. J. **846**, 168 (2017).
[34] A. Kaiser, J. Postler, M. Ončák, M. Kuhn, M. Renzler, S. Spieler, M. Simpson, M. Gatchell, M. K. Beyer, R. Wester, F. A. Gianturco, P. Scheier, F. Calvo, and E. Yurtsever, J. Phys. Chem. Lett. **9**, 1237 (2018).
[35] L. Tiefenthaler, J. Ameixa, P. Martini, S. Albertini, L. Ballauf, M. Zankl, M. Goulart, F. Laimer, K. von Haeften, F. Zappa, and P. Scheier, Rev. Sci. Instrum. **91**, 033315 (2020).
[36] S. Ralser, J. Postler, M. Harnisch, A. M. Ellis, and P. Scheier, Int. J. Mass Spectrom. **379**, 194 (2015).
[37] C. Leidlmair, Y. Wang, P. Bartl, H. Schobel, S. Denifl, M. Probst, M. Alcami, F. Martin, H. Zettergren, K. Hansen, O. Echt, and P. Scheier, Phys. Rev. Lett. **108**, 076101 (2012).
[38] M. Harnisch, N. Weinberger, S. Denifl, P. Scheier, and O. Echt, Mol. Phys. **113**, 2191 (2015).
[39] L. F. Gomez, E. Loginov, R. Sliter, and A. F. Vilesov, J. Chem. Phys. **135**, 154201 (2011).
[40] N. B. Brauer, S. Smolarek, E. Loginov, D. Mateo, A. Hernando, M. Pi, M. Barranco, W. J. Buma, and M. Drabbels, Phys. Rev. Lett. **111**, 153002 (2013).
[41] C. Mundo, M. Sommerfeld, and C. Tropea, Int. J. Multiphase Flow **21**, 151 (1995).
[42] J. Palacios, J. Hernandez, P. Gomez, C. Zanzi, and J. Lopez, Exp. Therm. Fluid. Sci. **44**, 571 (2013).
[43] F. Laimer, F. Zappa, P. Scheier, and M. Gatchell, Chemistry **27**, 7283 (2021).
[44] D. A. Thomas, E. Mucha, M. Lettow, G. Meijer, M. Rossi, and G. von Helden, J. Am. Chem. Soc. **141**, 5815 (2019).
[45] J. Fulara, M. Jakobi, and J. P. Maier, Chem. Phys. Lett. **211**, 227 (1993).